Journal of Solid State Chemistry 182 (2009) 2486–2490

Contents lists available at ScienceDirect

Journal of Solid State Chemistry

journal homepage: www.elsevier.com/locate/jssc

Fabrication of a graphene–cuprous oxide composite

Chao Xu [a], Xin Wang [a,*], Lichun Yang [b], Yuping Wu [b]

[a] Key Laboratory for Soft Chemistry and Functional Materials of Ministry Education, Nanjing University of Science and Technology, Nanjing 210094, China
[b] Department of Chemistry and Shanghai Key Laboratory of Molecular Catalysis and Innovative Materials, Fudan University, Shanghai 200433, China

ARTICLE INFO

Article history:
Received 11 May 2009
Received in revised form
29 June 2009
Accepted 1 July 2009
Available online 8 July 2009

Keywords:
Graphene
Cu_2O cubes
Adsorption
Reduction
Composite

ABSTRACT

A composite of graphene–cuprous oxide (Cu_2O) was prepared using copper acetate-adsorbed graphene oxide (GO) sheets as precursors. In this composite, in-situ formed Cu_2O particles were derived from the adsorbed copper acetate which attached to graphene sheets and prevented the aggregation of the reduced graphene oxide sheets. The as-synthesized Cu_2O crystals were cube-like particles distributed randomly on the sheets due to the template effect of GO, consequently forming a graphene–Cu_2O cubes composite. A preliminary study on the electrochemical behavior of the graphene–Cu_2O composite used as anode material for lithium ion batteries was carried out.

1. Introduction

Graphene-based materials are quite intriguing from the perspectives of both fundamental science and technology [1–5]. Due to their unique nanostructure and extraordinary properties, graphene-based materials are attractive as nanoscale building block for the synthesis of graphene-based composites [6]. For example, integration of graphene and certain functional particles has presented unique features in the new hybrids which have potential applications in catalysis, biosensors, methanol fuel cells, and optics [7–12].

Cuprous oxide (Cu_2O) is attracting more and more research attention for its potential applications in hydrogen production, solar energy, catalysis, and anode material for lithium ion batteries [13–15]. Apart from some research on the morphology of Cu_2O [14,15], several studies have been performed regarding the integration of Cu_2O on carbonaceous materials to obtain enhanced properties for applications, such as the stable catalytic activity of carbon nanotubes-Cu_2O cathodes in water treatment [16–18]. It is known that graphene is a burgeoning pseudo-two-dimensional carbonaceous nanosheet possessing special intrinsic properties [1,4]. Thus, the combination of graphene and Cu_2O may display some unique properties useful in practical applications.

As recently demonstrated, graphene can be obtained in bulk by chemical reduction of graphene oxide, e.g. using ethylene glycol as reductant [7,19]. Usually, the van der Waals interactions between these reduced graphene oxide sheets made them restack to form graphite [20,21]. Attachment of additions, such as polar molecules and polymers, on graphene oxide during the reduction process can reduce the aggregation of these graphene sheets [3,20,22]. Based on this methodology, we used copper acetate pre-adsorbed graphene oxide sheets to prepare graphene-based composite in ethylene glycol system (Fig. 1). Additionally, ethylene glycol has also been used as both solvent and reductant in preparing Cu_2O [15,17]. Thus, the attached copper acetate may not only prevent the restacking of the graphene sheets during the reduction process, but also can be reduced into Cu_2O, consequently forming a graphene–Cu_2O composite. It was found that in this composite, the reduced graphene oxide sheets were almost exfoliated and were decorated randomly by Cu_2O particles. Interestingly, it was easy to obtain cube-like Cu_2O particles in the composite probably due to the template effect of the carbon sheets, while only aggregation of Cu_2O could be obtained in the absence of graphene oxide. We used the as-synthesized composite as an anode material for lithium ion batteries to evaluate its electrochemical properties, and the results showed that the composite delivered a high capacity in the first charge–discharge cycle, indicating potential applications in high-capacity batteries or capacitors.

2. Experimental section

2.1. Preparation of graphene–Cu_2O composite

Graphite oxide (GO) was prepared according to the method reported by Hummers and Offeman [23] from purified natural graphite bought from Qingdao Zhongtian Company with a mean particle size of 44 μm. The synthesis of the graphene–Cu_2O

* Corresponding author. Fax: +86 25 84315943.
E-mail address: wxin@public1.ptt.js.cn (X. Wang).

0022-4596/$ - see front matter © 2009 Elsevier Inc. All rights reserved.
doi:10.1016/j.jssc.2009.07.001

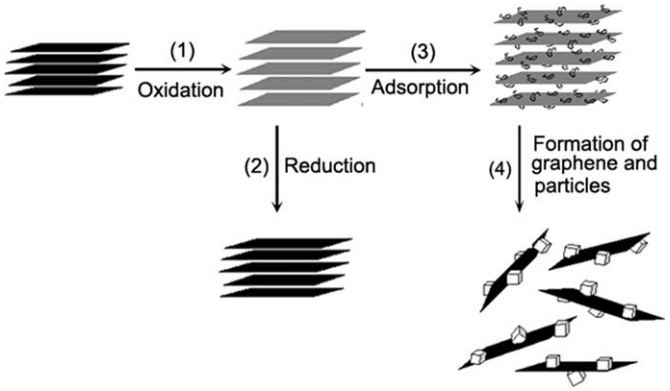

Fig. 1. A proposed scheme of the formation of graphene and graphene–Cu_2O composites. (1) Oxidation of graphite (black blocks) to graphite oxide (lighter colored blocks) with greater interlayer distance. (2) Direct reduction of graphite oxide with reductant. (3) Absorption of copper acetate on the graphene oxide sheets. (4) Formation of graphene-supported Cu_2O particles by the reduction of graphene oxide sheets and the in-situ crystal growth of Cu_2O. The distorted carbon sheets are simplified to an idealized planar model.

composite involved two steps. In the first step, 60 mg of copper acetate ($Cu(Ac)_2$) and 100 mg of GO were dispersed into 200 mL of absolute ethanol with sonication for 2 h. The mixture was magnetically stirred for 4 h, and then centrifuged and washed copiously with ethanol. The obtained sample was dried at 60 °C for 8 h and labeled as GO–$Cu(Ac)_2$. In the second step, 50 mg of GO–$Cu(Ac)_2$ composite was mixed with 50 mL of ethylene glycol under sonication in a 100 mL round-bottomed flask for 0.5 h, and the resulting mixture was heated to 140 °C under vigorous magnetic stirring. Subsequently, 2.5 mL of distilled water was added, and the mixture was heated at 160 °C for 2 h. After the system was cooled to room temperature, the suspension was centrifuged, washed by absolute ethanol five times to remove the remaining ethylene glycol and soluble by-products, and dried in a vacuum oven at 60 °C for 6 h. The product was labeled as G–Cu_2O. Additionally, Cu_2O and GO were synthesized with the same parameters for comparison.

2.2. Characterization

The dried products were characterized by X-ray diffraction (XRD) on a Bruker D8 Advance diffractometer with Cu $K\alpha$ radiation at a slow scan rate of 0.02°/s to determine the structure. Fourier-transform infrared spectroscopy (FT-IR) analyses were carried out on a Bruker Vector-22 spectrophotometer using a potassium bromidepellet technique. Transmission electron microscopy (TEM) analyses were taken with a JEOL JEM2100 microscope. Scanning electron microscopy (SEM) analyses were carried out on a JEOL JSM-6380LV scanning electron microscope equipped with an energy-dispersive X-ray spectrometer (EDS). Samples for atomic force microscopy (AFM) imaging were prepared by dispersing the composite in ethanol under sonication, followed by depositing dispersions of hybrid on a freshly cleaved mica surface, which were then allowed to dry in air at room temperature. AFM images were taken on a SPI3800N scanning probe microscope, and imaging was done in non-contact mode. The content of Cu_2O in composite was analyzed on an IRIS Intrepid II XSP.

Electrochemical performance of the electrodes was evaluated by assembling model coin-type cells using lithium foil as a counter and reference electrode, Celgard 2400 as a separator, and 1 M $LiPF_6$ solution in ethylene carbonate/dimethyl carbonate/diethyl carbonate (1:1:1, w/w%) as an electrolyte. Capacity measurements for samples were carried out at 0.1 mA cm^{-1} in the voltage range of 0–3 V. The working electrodes were prepared by mixing active material, acetylene black and poly(vinylidene fluoride) at a ratio of 85:10:5 (w/w%). The mixture was coated onto a copper foil. After drying, the coated foils were cut into pellets. Prior to assembling into coin-type model cells under argon atmosphere in a glove box, all the electrode pellets were dried overnight under vacuum at 120 °C.

3. Results and discussion

As a result of the introduction of oxygen-containing functional groups (hydroxyl, carboxyl and epoxy groups) on graphene nanosheets, GO could easily adsorb polar molecules or polymers via the functional groups as anchors [24,25]. In fact, GO can also adsorb metal salts such as copper acetate on its surface. As shown in Fig. 2(a), the characteristic features in the FT-IR spectrum of GO are the absorption bands corresponding to the C=O carbonyl stretching at 1720 cm^{-1}, the C–OH stretching at 1224 cm^{-1}, the C–O stretching at 1050 cm^{-1}, and the remaining sp2 character at 1620 cm^{-1} [25]. After mixing the two components, the FT-IR spectrum of the hybrid becomes a combination of the absorption bands of GO and $Cu(Ac)_2$ [26]. Apart from the signals of $Cu(Ac)_2$, the absorption bands at 1720 and 1620 cm^{-1} (a shoulder peak) are attributed to GO (Fig. 2(c)) [27]. Additionally, the absorption bands of carbonyl of the copper acetate shifting from 1600 to 1560 cm^{-1} and the broadened peaks appearing around 1100 cm^{-1} both indicate that there is a strong interaction between copper acetate and GO [17]. After adsorption of $Cu(Ac)_2$ molecules on graphene oxide sheets, the interlayer spacing of the dried GO broadened [28]. By comparing the XRD patterns of GO and GO–$Cu(Ac)_2$ in Fig. 3, it may be clearly observed that the interlayer spacing of GO (1.03 nm) in GO–$Cu(Ac)_2$ is larger than that of the starting GO (0.82 nm).

Fig. 4 shows the SEM images and the EDS analyses of GO and GO–$Cu(Ac)_2$. As the arrow shows in Fig. 4(b), the layered structure of GO still remains in the pre-intercalated product, and this result is consistent with that of the XRD measurements. It is expected that the chemical composition of GO–$Cu(Ac)_2$ should be different from that of the pure GO. EDS analyses revealed that the composition of GO sheets mostly consisted of C and O, while that of the GO–$Cu(Ac)_2$ contained not only C and O, but also the Cu

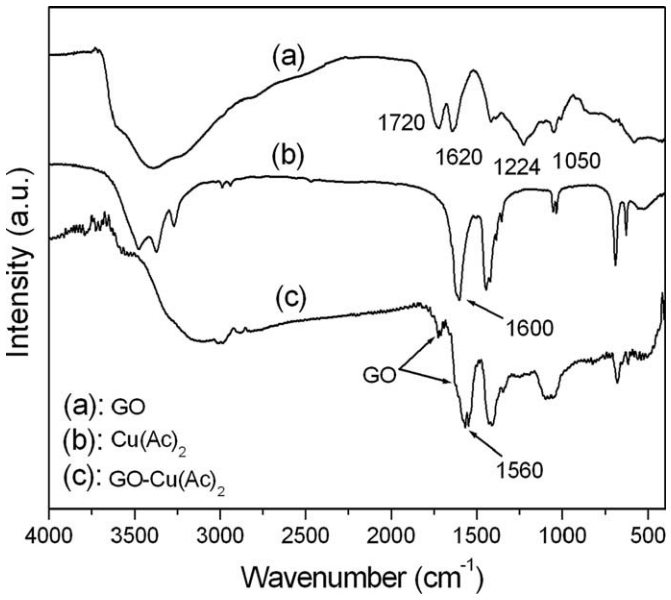

Fig. 2. FT-IR spectra of (a) GO, (b) $Cu(Ac)_2$ and (c) GO–$Cu(Ac)_2$ hybrid.

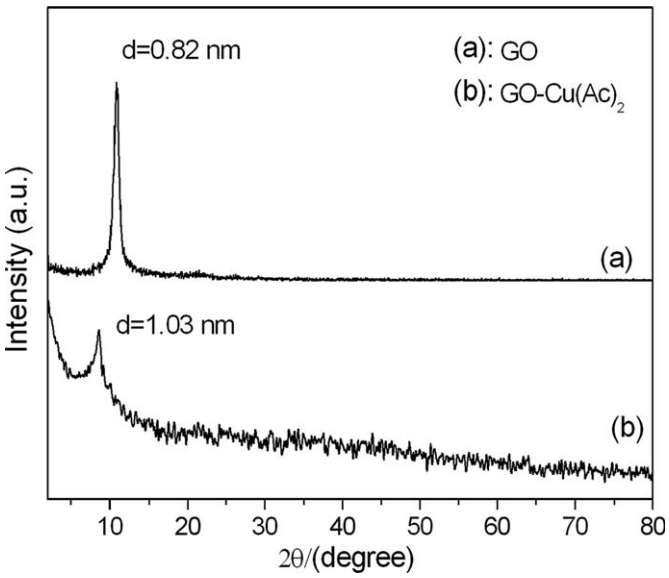

Fig. 3. XRD patterns of (a) GO and (b) GO–$Cu(Ac)_2$.

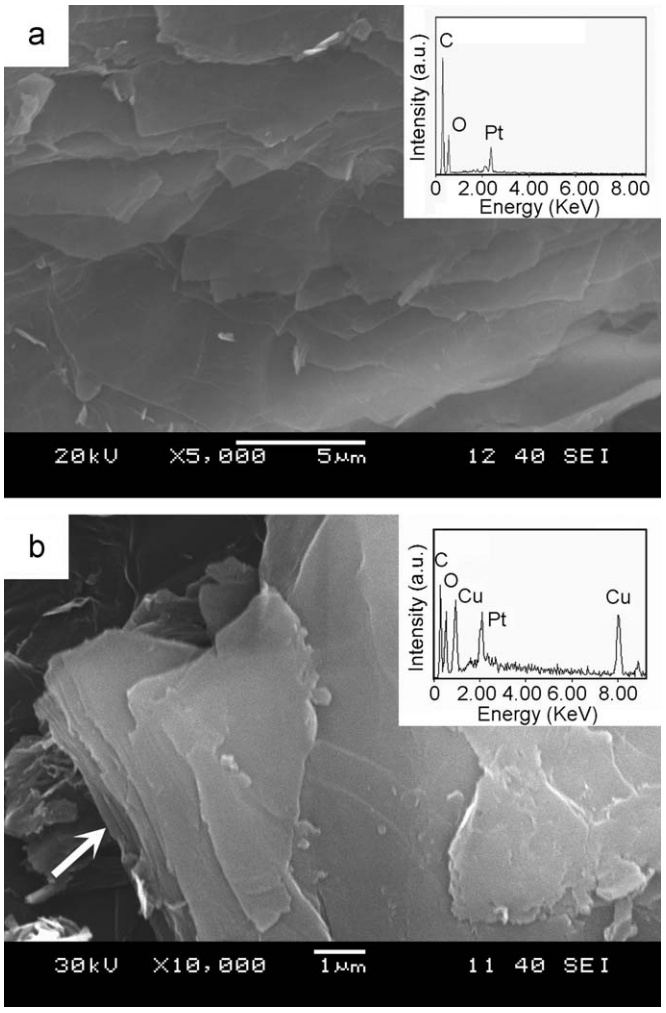

Fig. 4. SEM images and EDS spectra of (a) GO and (b) GO–$Cu(Ac)_2$ hybrid. The Pt signals come from the plated element.

element (see insert images in Fig. 4(a) and (b)). Thus, according to above experimental results, pre-intercalated GO with copper acetate was obtained. It is believed that the strong attachment of molecules on GO will be beneficial for the exfoliation of graphene sheets during the reduction process [20].

GO can be reduced by ethylene glycol and the synthesized graphene sheets can restack to form poorly ordered graphite along the stacking direction (Fig. 5(b)). (The details on reduction of GO with ethylene glycol can found in Ref. [19] and Supplementary Information.) As shown in Fig. 5(a), however, after treating the GO–$Cu(Ac)_2$ hybrid with ethylene glycol, the reflection peaks (0 0 2) of layered graphite almost disappeared (see Fig. 5(b)) and the diffraction peaks of composite are in good agreement with those of pure Cu_2O with cubic phase (JCPDS78-2076). Previous studies by our team and other groups have shown that if the regular stack of GO or graphite is broken—for example exfoliation, their diffraction peaks may also become weak or even disappear [7,30]. In addition, due to the relatively lower weight content of Cu_2O in the composite (about 20%), the diffraction signals of Cu_2O may not cover up that of the carbon sheets [7,31]. Therefore, we surmised that the in-situ formed Cu_2O through the polyol process [15,29] might attach onto these carbon sheets and prevent the aggregation and restack of these as-synthesized graphene, which weakens the diffraction of single layered carbon sheets consequently (Fig. 1) [7,11]. Further evidence for this conjectural structure can be supported by the morphological analyses.

Fig. 6(a) shows a typical TEM image of G–Cu_2O composite. It can be clearly seen that the graphene sheets are decorated by cubic Cu_2O particles with an edge length of 100–250 nm. These cubic crystals are distributed randomly on the surface and edges of the graphene sheets, just like the particles adhering to Scotch tape (Fig. 5S, Supplementary Information) [17]. Previous studies have shown that graphite oxide can be exfoliated in ethylene glycol, thus these graphene oxide sheets with adsorbed $Cu(Ac)_2$ can also form stable dispersion in ethylene glycol [32]. After reduction by ethylene glycol, the as-synthesized Cu_2O particles anchored on these graphene-based sheets, forming hybrid

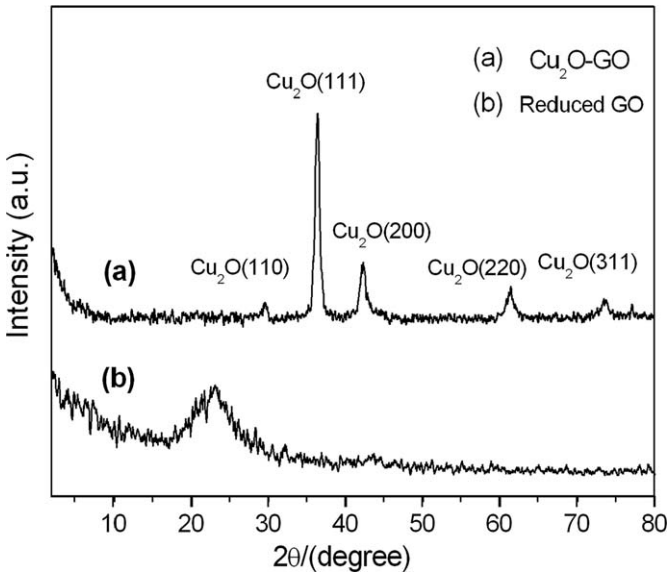

Fig. 5. The XRD patterns. (a) G–Cu_2O composite. The peaks at $2\theta = 29^\circ$, 37°, 41°, 62° and 74° are assigned to (1 1 0) (1 1 1), (2 0 0), (2 2 0) and (3 1 1) crystalline planes of Cu_2O, which indicates that the particles are composed of pure crystalline Cu_2O. (b) As-reduced GO under the same conditions. The characteristic peak (0 0 2) of graphite is broader than that of original graphite due to the poor order of the stacked graphite.

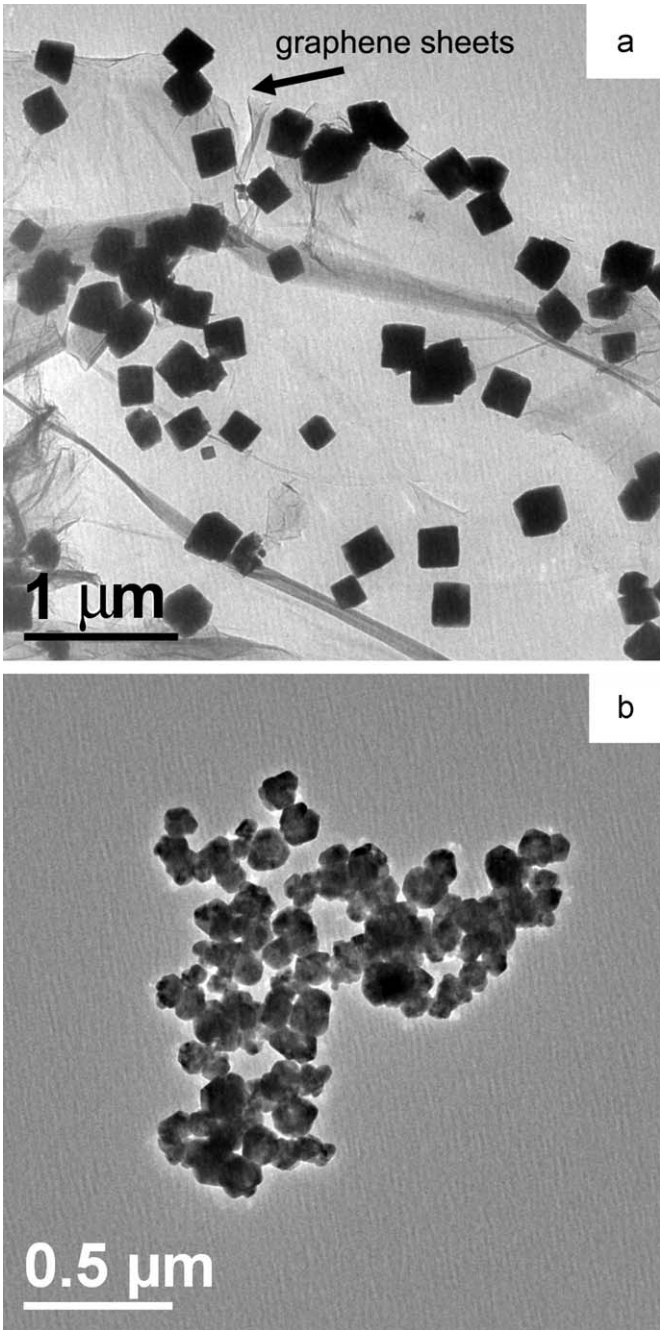

Fig. 6. TEM images of (a) G–Cu_2O composite and (b) the as-synthesized Cu_2O crystals in the absence of GO.

composite consequently. Additionally, it is worth noting that when we used this same method to synthesize Cu_2O without GO, only the non-cubic Cu_2O particles were obtained (Fig. 6(b)). Recently, there has been much research on the synthesis of Cu_2O cubes, and the different formation mechanisms were used to explain this process [14,33,34]. It should be pointed out that in our system without any surfactants, the cubic Cu_2O particles were obtained, while these cubes were hardly found in the presence of other carbonaceous materials such as carbon nanotubes [17,35]. We assume that in our system the carbon sheets may play a role as a template which makes Cu_2O crystals grow along certain directions, forming cube-like crystals. The exact role of carbon sheets in this process and the formation mechanism of cubic Cu_2O itself still await further studies.

The representative SEM images of the composite also reveal a structural feature which is consistent with the above discussion. In Fig. 7, it can be clearly seen that the cubic Cu_2O crystals are randomly distributed on graphene sheets, while the cubes lie between the graphene sheets may be attributed to the restacking of the graphene–Cu_2O composite (the ring as shown in Fig. 7(a)) [32]. In addition, it was also observed that some of cubic Cu_2O was loosely inserted into the carbon sheets, but not attached to the surface (see the arrows show in Fig. 7(b)). The structural analyses suggested that holes and defects are easily produced on the carbon grid through the chemical conversion of graphite oxide to graphene [36,37]. Thus it is possible that the Cu_2O crystals grow around these holes and defects, and are inclined to insert into these sheets [17]. Additionally, the rigid particles may also easily sink into the fluff supported materials. As the AFM image shows in the Supplementary information, some of cubic Cu_2O seems partially inserted into a soft support material (graphene sheets), which is in accordance with the SEM results.

As a new kind of carbonaceous material, graphene possesses excellent intrinsic properties and has been utilized as a promising supporting material to disperse and stabilize inorganic nanoparticles for potential applications in catalysis, biosensors and other nanotechnologies [7,9]. It is expected that the integration of graphene with Cu_2O cubes may lend itself to a new material with special properties useful in some potential applications [37]. As a preliminary study, we used a graphene–Cu_2O composite as an anode material in lithium ion batteries and found that the

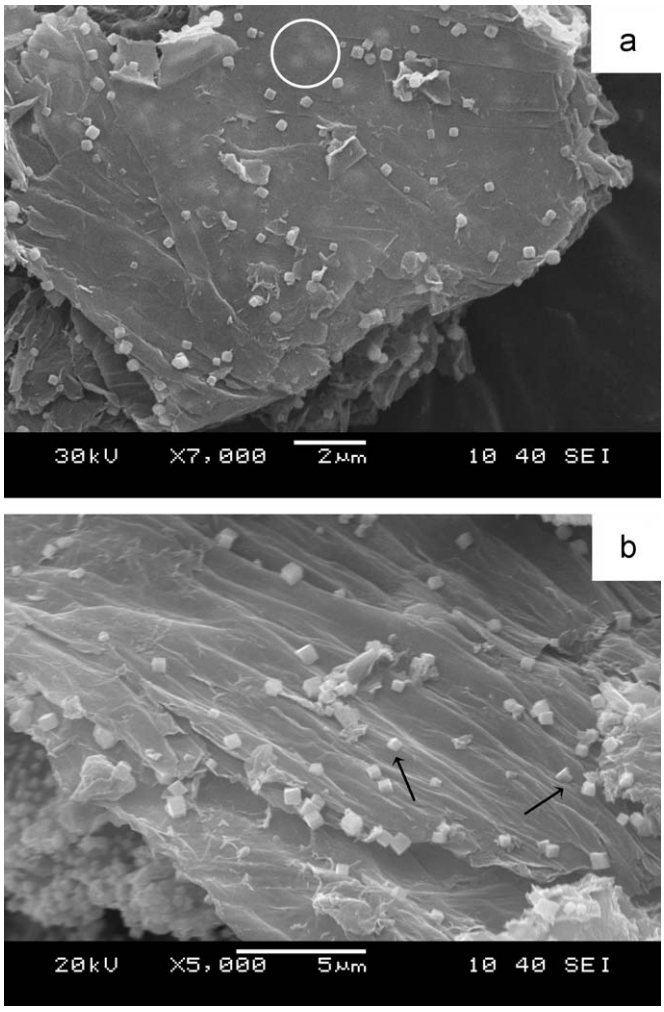

Fig. 7. SEM images of GO–Cu_2O composite.

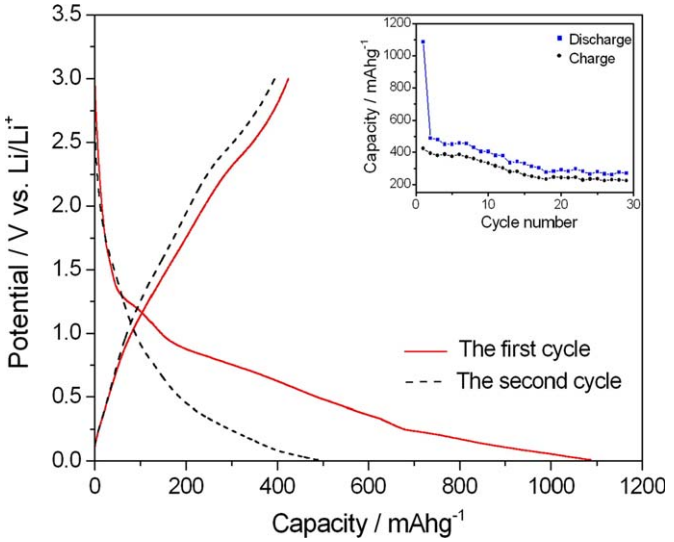

Fig. 8. Electrochemical properties of G–Cu_2O as electrode materials in lithium ion batteries: The first and second charge–discharge cycles. The inset is the charge and discharge capacities in different cycles.

capacity of the sample was ca.1100 mAh/g in the first charge–discharge cycle (as shown in Fig. 8), which is higher than that of graphene [5,38] or Cu_2O cubes [39]. Nevertheless, the electrode showed a poor cyclability. Although the exact mechanisms for the storage of lithium in graphene or graphene–Cu_2O composites are unclear and a number of problems remain to be solved before practical use [5,39], we believe that these graphene-based materials are promising anode materials for high-capacity lithium ion batteries in the near future.

4. Conclusion

In summary, we have demonstrated that a graphene–Cu_2O composite can be synthesized using modified graphene oxide sheets as precursors in the solution approach. The synthesis procedure can be divided into two steps: the formation of pre-intercalated GO by $Cu(Ac)_2$, followed by the reduction of graphene oxide and the in-situ crystal formation of Cu_2O particles between the layers. The experimental results show that the lamellar graphene sheets in this composite are exfoliated by the in-situ crystals growth and are decorated randomly by these as-formed Cu_2O particles. Meanwhile, the as-synthesized graphene sheets may affect the crystal orientation of Cu_2O particles and make these crystals grow along a certain orientation forming cube-like particles with an average edge length of about 200 nm. And the special capacity of graphene–Cu_2O composite indicates its potential application in batteries and capacitors in the future.

Supplementary information

Electronic Supplementary Information (ESI) available: XRD patterns of graphite and the reduced graphite oxide; FT–IR spectra, XPS spectra and TGA curves of graphite oxide and the reduced graphite oxide; AFM image and FT–IR spectra of G–Cu_2O.

Acknowledgements

Financial support from the National Natural Science Foundation of China (No.10776014) and the High Technology Foundation of Jiangsu Province (No.BG(2007)047) is greatly appreciated.

Appendix A. Supporting Information

Supplementary data associated with this article can be found in the online version at doi:10.1016/j.jssc.2009.07.001.

References

[1] A.K. Geim, K.S. Novoselov, Nat. Mater. 6 (2007) 183–191.
[2] J.C. Meyer, A.K. Geim, M.I. Katsnelson, K.S. Novoselov, T.J. Booth, S. Roth, Nature 446 (2007) 60–63.
[3] S. Stankovich, D.A. Dikin, G.H.B. Dommett, K.M. Kohlhaas, E.J. Zimney, E.A. Stach, R.D. Piner, S.T. Nguyen, R.S. Ruoff, Nature 442 (2006) 282–286.
[4] T. Ramanathan, A.A. Abdala, S. Stankovich, D.A. Dikin, M. Herrera-Alonso, R.D. Piner, D.H. Adamson, H.C. Schniepp, X. Chen, R.S. Ruoff, S.T. Nguyen, I.A. Aksay, R.K. Prud'Homme, L.C. Brinson, Nat. Nanotechnol. 3 (2008) 327–331.
[5] E.J. Yoo, J. Kim, E. Hosono, H.S. Zhou, T. Kudo, I. Honma, Nano Lett. 8 (2008) 2277–2282.
[6] D. Li, R.B. Kaner, Science 320 (2008) 1170–1171.
[7] C. Xu, X. Wang, J.W. Zhu, J. Phys. Chem. C 112 (2008) 19841–19845.
[8] R. Muszynski, B. Seger, P.V. Kamat, J. Phys. Chem. C 112 (2008) 5263–5266.
[9] G. Williams, B. Seger, P.V. Kamat, ACS Nano 2 (2008) 1487–1491.
[10] J. Lu, I. Do, L.T. Drzal, R.M. Worden, I. Lee, ACS Nano 2 (2008) 1825–1832.
[11] C. Xu, X. Wang, J. Zhu, X.J. Yang, L.D. Lu, J. Mater. Chem. 18 (2008) 5625–5629.
[12] B.S. Kong, J.X. Geng, H.T. Jung, Chem. Commun. 16 (2009) 2174–2176.
[13] H.G. Zhang, Q.S. Zhu, Y. Zhang, Y. Wang, L. Zhao, B. Yu, Adv. Funct. Mater. 17 (2007) 2766–2771.
[14] L.F. Gou, C.J. Murphy, Nano Lett. 3 (2003) 231–234.
[15] Z.C. Orel, A. Anzlovar, G. Drazic, M. Zigon, Crystal Growth Des. 7 (2007) 453–458.
[16] Z.H. Ai, H.Y. Xiao, T. Mei, J. Liu, L.Z. Zhang, K.J. Deng, J.R. Qiu, J. Phys. Chem. C 112 (2008) 11929–11935.
[17] Y. Yu, L.L. Ma, W.Y. Huang, F.P. Du, J.C. Yu, J.G. Yu, J.B. Wang, P.K. Wong, Carbon 43 (2005) 670–673.
[18] L.J. Fu, J. Gao, T. Zhang, Q. Cao, L.C. Yang, Y.P. Wu, R.J. Holze, Power Sources 171 (2007) 904–907.
[19] C. Nethravathi, M. Rajamathi, Carbon 46 (2008) 1994–1998.
[20] D. Li, M.B. Muller, S. Gilje, R.B. Kaner, G.G. Wallace, Nat. Nanotechnol. 3 (2008) 101–105.
[21] G.X. Wang, J. Yang, J. Park, X.L. Gou, B. Wang, H. Liu, J. Yao, J. Phys. Chem. C 112 (2008) 8192–8195.
[22] S. Stankovich, R.D. Piner, X. Chen, N. Wu, S.T. Nguyen, R.S. Ruoff, J Mater. Chem. 16 (2006) 155–158.
[23] W.S. Hummers, R.E. Offeman, J. Am. Chem. Soc. 80 (1958) 1339.
[24] C. Xu, X.D. Wu, J.W. Zhu, X. Wang, Carbon 46 (2008) 386–389.
[25] M. Herrera-Alonso, A.A. Abdala, M.J. McAllister, I.A. Aksay, R.K. Prud'homme, Langmuir 23 (2007) 10644–10649.
[26] Y. Matsuo, K. Hatase, Y. Sugie, Chem. Mater. 10 (1998) 2266–2269.
[27] A.B. Bourlinos, D. Gournis, D. Petridis, T. Szabo, A. Szeri, I. Dekany, Langmuir 19 (2003) 6050–6055.
[28] H.K. Jeong, Y.P. Lee, R. Lahaye, M. Park, K.H. An, I.J. Kim, C. Yang, C.Y. Park, R.S. Ruoff, Y.H. Lee, J. Am. Chem. Soc. 130 (2008) 1362–1366.
[29] J.W. Zhu, Y.P. Wang, X. Wang, X.Y. Yang, L.D. Lu, Powder Technol. 181 (2008) 249–254.
[30] D. Cai, M. Song, J. Mater. Chem. 17 (2007) 3678–3680.
[31] J. Li, S.B. Tang, L. Lu, H.C. Zeng, J. Am. Chem. Soc. 129 (2007) 9049–9401.
[32] J.I. Paredes, S. Villar-Rodil, A. Martinez-Alonso, J.M.D. Tascon, Langmuir 24 (2008) 10560–10564.
[33] D.B. Wang, M.S. Mo, D.B. Yu, L.Q. Xu, F.Q. Li, Y.T. Qian, Crystal Growth Des. 3 (2003) 717–720.
[34] M.H. Kim, B. Lim, E.P. Lee, Y.N. Xia, J. Mater. Chem. 18 (2008) 4069–4073.
[35] Y. Yu, L.L. Ma, W.Y. Huang, J.L. Li, P.K. Wong, J.C. Yu, J. Solid State Chem. 178 (2005) 1488–1494.
[36] M.J. McAllister, J.L. Li, D.H. Adamson, H.C. Schniepp, A.A. Abdala, J. Liu, M. Herrera-Alonso, D.L. Milius, R. Car, R.K. Prud'homme, I.A. Aksay, Chem. Mater. 19 (2007) 4396–4404.
[37] K.N. Kudin, B. Ozbas, H.C. Schniepp, R.K. Prud'homme, I.A. Aksay, R. Car, Nano Lett. 8 (2008) 36–41.
[38] F.Y. Cheng, Z.L. Tao, J. Liang, J. Chen, Chem. Mater. 20 (2008) 667–681.
[39] C.Q. Zhang, J.P. Tu, X.H. Huang, Y.F. Yuan, X.T. Chen, F.J. Mao, Alloys Compd. 441 (2007) 52–56.